3Dwheel: 3-Axis Low Noise, High-Bandwidth Attitude Actuation from a Single Momentum Wheel Using Magnetic Bearings

Jon Seddon, Alexandre Pechev
Surrey Space Centre
University of Surrey, Guildford, GU2 7XH, UK; +44 (0)1483 683411
j.seddon@surrey.ac.uk, a.pechev@surrey.ac.uk

ABSTRACT

This paper proposes a new concept for attitude actuation for small satellites that uses active magnetic bearings to support and tilt a spinning rotor to provide 3-axis attitude control of the satellite using a single actuator. A controlled 3D motion in the spinning rotor provides a conventional torque output about the momentum axis and a gyroscopic torque output about any direction in the plane normal to the spinning axis. Therefore, a single tilting momentum-wheel can generate torque along the three principal axes of the satellite, providing mass and power savings, or redundancy.

In this paper we present a model of, and results from the engineering model that has been built of the tilting magnetically-levitated momentum-wheel. The control loop that levitates and tilts the rotor is discussed. The 3-axis actuation of this wheel is demonstrated with simulations of the wheel fitted to the TopSat small satellite. The bandwidth and torque output of the wheel are compared with a conventional momentum wheel's. The power consumption, operation and stiffness of the magnetic bearing are discussed. The 2.5 micrometre translational and 0.1 milliradian rotational control of the wheel obtained in experiments with the engineering model are demonstrated.

INTRODUCTION

Active Magnetic Bearings (AMBs) are increasingly being used as they have many desirable properties compared to conventional roller or ball bearings. AMBs eliminate all contact between moving parts, preventing friction, stiction and wear. Because there is no contact there is no need for lubrication, making them especially useful for use in the vacuum of space. Because of the lack of friction the spin rate of the bearing can be increased. The lack of friction will also increase the lifetime of the bearing and reduce its sensitivity to temperature. The active control of the rotor position minimises wheel jitter and makes for a very low noise bearing. There are however some disadvantages such as an increase in the complexity of the system, and an increase in power consumption due to the electromagnets, although the spin motor power consumption is reduced because of the elimination of friction and stiction.

The use of AMBs also allows the rotor to be tilted through a small range of angles if properly designed, giving it some additional properties. A conventional output torque can be generated about the rotor's spin axis and a gyroscopic torque can be generated about any axis in the plane normal to the spin axis. The AMBs allow the rotor to be tilted at a high angular rate, generating a large gyroscopic torque. Because the axis of the gyroscopic torque can be controlled, we propose a single tilting momentum wheel that can generate an output torque about all three axes of the spacecraft. The bandwidth of the output torque is very high making it ideal for the damping of vibrations and rapid reorientation of the spacecraft, for instance in rendezvous and docking procedures.

The rotor can only be tilted through a small range of angles. The range of angles is limited by the width of the airgap between the electromagnet pole face and the rotor. A large airgap reduces the magnetic flux in the airgap and so decreases the stiffness of the bearing and increases the power consumption. Finite element simulations show that a tilt range of $\pm 3^\circ$ is feasible. Because the tilt range is small and the tilt rate is high then this gyroscopic torque can only be generated for a short time. This makes the gyroscopic torque more suitable for the damping of high frequency disturbances, or for high bandwidth small-angle manoeuvres, such as in satellite rendezvous and docking.

This paper discusses the theory behind the use of AMBs in a spacecraft momentum wheel. A mathematical model of a tilting magnetically-levitated momentum-wheel is derived. A controller to stabilise the wheel is generated and the performance and properties of the wheel are simulated and discussed.

In this paper we then present experimental data from an engineering model of the wheel that has been built. The translational position of this wheel can be controlled with an accuracy of 2.5 micrometres and the tilt angle can be controlled with an accuracy of 0.1 milliradians. The bandwidth of the wheel and controller is 176 rads^{-1} and so can counteract high frequency disturbances as predicted by the simulations. The limitation in rotational and translational position is due to the resolution of the sensors.

SYSTEM MODEL

Prior magnetically-levitated momentum-wheels for spacecraft have used the electrodynamic principle[1,2,3], where permanent magnets generate bias flux in the magnetic bearing and actively controlled electromagnets generate a control flux to stabilise the system. This system has the advantage of having a linear relationship between the force acting on the rotor and the applied current[4]. The alternative approach taken by the authors uses the electromagnetic principle where a purely attractive force acting on the rotor is generated by electromagnets. This approach has the benefit of being able to generate larger forces, increasing the stiffness of the bearing if required[5].

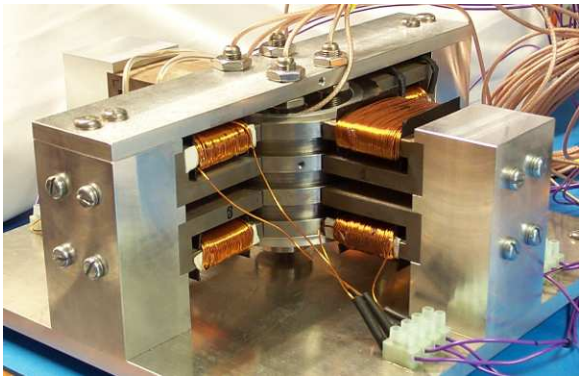

Figure 1: The Engineering Model of the Wheel

Figure 1 shows the arrangement of the electromagnets around the rotor in our design. The geometry of the rotor and electromagnets was optimised with the use of three-dimensional magnetostatic finite element simulations. The centre of the inertial co-ordinate system is at the geometrical centre of the rotor. x, y and z are the translational distance that the rotor has been displaced from its central position along the principal inertial axes. α_x, α_y and α_z are the angles that the rotor has been rotated about the principal inertial axes from its central position. The electromagnets are aligned along the positive and negative inertial axes.

The attractive reluctance force generated by the i-th electromagnet is given by[6]

$$f_i = -\frac{\mu_0 N^2 \varepsilon l i^2}{4\gamma^2} \tag{1}$$

where μ_0 is the permeability of free space, N is the number of terms in the electromagnet coil, εl is the cross sectional area of the electromagnet pole face, i is the current flowing through the coils and γ is the width of the airgap between the electromagnet pole face and the rotor pole face. The negative sign is to indicate that the reluctance force is attractive. The kinematics to map the force generated by each of the electromagnets to the total force acting on the rotor are

$$\begin{bmatrix} F_x \\ F_y \\ F_z \end{bmatrix} = \begin{bmatrix} 1 & 1 & 0 & 0 & -1 & -1 & 0 & 0 \\ 0 & 0 & 1 & 1 & 0 & 0 & -1 & -1 \\ 0 & 0 & 0 & 0 & 0 & 0 & 0 & 0 \end{bmatrix} \begin{bmatrix} f_1 \\ f_2 \\ f_3 \\ f_4 \\ f_5 \\ f_6 \\ f_7 \\ f_8 \end{bmatrix} \tag{2}$$

where $F = [F_x F_y F_z]^T$ is the force acting on the rotor along the principal inertial axes and f_1 to f_8 are the attractive forces generated by the eight electromagnets. The kinematic mapping between electromagnet forces and the torque on the rotor is given by

$$\begin{bmatrix} T_x \\ T_y \\ T_z \end{bmatrix} = r_z \begin{bmatrix} 0 & 0 & -1 & 1 & 0 & 0 & 1 & -1 \\ 1 & -1 & 0 & 0 & -1 & 1 & 0 & 0 \\ 0 & 0 & 0 & 0 & 0 & 0 & 0 & 0 \end{bmatrix} \begin{bmatrix} f_1 \\ f_2 \\ f_3 \\ f_4 \\ f_5 \\ f_6 \\ f_7 \\ f_8 \end{bmatrix} \tag{3}$$

where $T = [T_x T_y T_z]^T$ is the torque acting about the three principal inertial axes and r_z is the length of the moment that the torques act about, which is the distance along the z-axis from the centre of the axes to the centre of the electromagnets.

The translational dynamic behaviour of the rotor is given by Newton's Second Law

$$ma = F \tag{4}$$

where F is the vector force acting on the rotor in the inertial reference frame and a is the acceleration of the rotor in the inertial reference frame. The rotational dynamics of the rotor are given by[7]

$$I\ddot{\alpha} + \dot{\alpha} \times I\dot{\alpha} = T + T_d \tag{5}$$

where T is the control torque acting on the rotor, T_d is the disturbance torque on the rotor, I is the inertia matrix of the rotor, $\dot{\alpha}$ is the angular velocity of the rotor about the principal axes and $\ddot{\alpha}$ is the angular acceleration of the rotor about the principal axes.

Equation 1 shows that the reluctance force generated by each electromagnet depends upon the width of the airgap of each electromagnet. This airgap depends upon the translational and rotational position of the rotor. Because of the small range considered, using small angle approximations and considering translation and rotation separately, the change in the airgap at each electromagnet can be calculated as

$$\begin{bmatrix} \triangle\gamma_1 \\ \triangle\gamma_2 \\ \triangle\gamma_3 \\ \triangle\gamma_4 \\ \triangle\gamma_5 \\ \triangle\gamma_6 \\ \triangle\gamma_7 \\ \triangle\gamma_8 \end{bmatrix} = \begin{bmatrix} -1 & 0 & 0 & -r_z \\ -1 & 0 & 0 & r_z \\ 0 & -1 & r_z & 0 \\ 0 & -1 & -r_z & 0 \\ 1 & 0 & 0 & r_z \\ 1 & 0 & 0 & -r_z \\ 0 & 1 & -r_z & 0 \\ 0 & 1 & r_z & 0 \end{bmatrix} \begin{bmatrix} x \\ y \\ \alpha_x \\ \alpha_y \end{bmatrix} \tag{6}$$

where $\triangle\gamma_1$ to $\triangle\gamma_8$ are the changes in the airgaps at the electromagnets. The airgap width with the rotor in its central position is γ_0 and so $\gamma_i = \gamma_0 + \triangle\gamma_i$.

The dynamics of the brushless DC motor spinning the rotor are approximated in the Laplace domain by

$$\ddot{\alpha_z}(s) = \frac{s i_{drive}(s)}{sK_l + K_D} \tag{7}$$

where i_{drive} is the drive current to the motor, and the inertia and damping gains K_l and K_D are taken for a typical brushless DC motor used in the laboratory, with values 1.07×10^{-2} and 0.1 respectively. The angular acceleration output by the motor is multiplied by the moment of inertia about the z-axis of the rotor (I_{zz} in the inertia matrix) to give the output torque of the spin axis motor. This output torque is added to the torque from the kinematic Equation 3 to give the total force acting on the rotor in Equation 5 of the rotational dynamics.

3-axis Torque Output From the Proposed New Wheel

The 3-axis output torque from the full wheel system T is the sum of the gyroscopic output torque from tilting the wheel T' and the conventional torque from changing the angular velocity of the spinning wheel T''. Because the rotor is only tilted through a small range of angles, we can use small angle approximations to say that there is no component of the gyroscopic torque about the z-axis and the conventional acceleration torque only has a component about the z-axis.

The output torque from tilting the rotor is generated by the same physical process as a Control Moment Gyro (CMG). Incorporating the small angle approximations mentioned above, it is given by

$$T' = \begin{bmatrix} \dot{\alpha}_x \\ \dot{\alpha}_y \\ 0 \end{bmatrix} \times h_0(\alpha_x, \alpha_y, \dot{\alpha}_z) \tag{8}$$

where h_0 is the angular momentum of the spinning rotor, and is a function of the rotor spin rate about the z-axis and the angle of the rotor about the x and y axes. The angular momentum when the rotor is not tilted is

$$H_0(\dot{\alpha}_z) = I \begin{bmatrix} 0 \\ 0 \\ \dot{\alpha}_z \end{bmatrix} \tag{9}$$

The rotation matrix to rotate $H_0(\dot{\alpha}_z)$ about the y-axis and then the x-axis can be calculated by

$$\begin{aligned} R_{xy} &= \begin{bmatrix} 1 & 0 & 0 \\ 0 & \cos\alpha_x & -\sin\alpha_x \\ 0 & \sin\alpha_x & \cos\alpha_x \end{bmatrix} \begin{bmatrix} \cos\alpha_y & 0 & \sin\alpha_y \\ 0 & 1 & 0 \\ -\sin\alpha_y & 0 & \cos\alpha_y \end{bmatrix} \\ &= \begin{bmatrix} \cos\alpha_y & 0 & \sin\alpha_y \\ \sin\alpha_x \sin\alpha_y & \cos\alpha_x & -\sin\alpha_x \cos\alpha_y \\ -\cos\alpha_x \sin\alpha_y & \sin\alpha_x & \cos\alpha_x \cos\alpha_y \end{bmatrix} \end{aligned} \tag{10}$$

Therefore the output torque from tilting the rotor is given by

$$T' = \begin{bmatrix} \dot{\alpha}_x \\ \dot{\alpha}_y \\ 0 \end{bmatrix} \times R_{xy} I \begin{bmatrix} 0 \\ 0 \\ \dot{\alpha}_z \end{bmatrix} \tag{11}$$

The output torque about the z-axis from the acceleration of the rotor is given by

$$T'' = I_{zz} \begin{bmatrix} 0 \\ 0 \\ \ddot{\alpha}_z \end{bmatrix} \tag{12}$$

The output torque from the tilting magnetically-levitated momentum-wheel is the sum of the torques from tilting and accelerating the rotor $T = T' + T''$.

The spacecraft is simulated using the model given in[8]. The spacecraft inertia matrix used was from the TopSat 120 kg small satellite built by Surrey Satellite Technology Ltd.

The model developed here assumes that the rotor is perfectly balanced. In reality, there will be a slight static imbalance where the centre of mass of the rotor is offset slightly from the geometrical centre of the rotor and a dynamic or couple imbalance where the axes of the moments of inertia are at a slight angle to the inertial axes. The static imbalance will generate a disturbance force on the rotor along an axis on the x-y plane that rotates around the z-axis as the rotor rotates. The couple imbalance will generate a disturbance torque about an axis that lies on the x-y plane that rotates about the z-axis as the rotor rotates[9]. The proposed 3Dwheel has the necessary degrees of freedom actively controlled to counteract these imbalances. The inertia matrix for the rotor has been assumed to be diagonal. Small angle approximations were used to calculate the output torque from the wheel. The electrical dynamics of the coils are not included in the model.

CONTROL ARCHITECTURE

For the control of a spacecraft using a single tilting magnetically-levitated momentum-wheel, we propose a two stage controller. The first outer controller calculates the necessary tilt axis and tilt angle from the commanded input torque. The second stage is a feedback controller to maintain the rotor at the desired tilt angle and spin rate.

To calculate the tilt angle required to generate the torque command demanded from the wheel, the gyroscopic output torque Equation 8 can be rearranged to calculate the desired tilt rate from the demanded torque. Using small angle approximations, components of the tilt torque about the z-axis are zero and the tilt rate commands are

$$\begin{bmatrix} \hat{\dot{\alpha}}_x \\ \hat{\dot{\alpha}}_x \end{bmatrix} = \frac{1}{I_{zz}\dot{\alpha}_z \cos\alpha_x \cos\alpha_y} \begin{bmatrix} 0 & -1 \\ 1 & 0 \end{bmatrix} \begin{bmatrix} \hat{T}_x \\ \hat{T}_y \end{bmatrix} \tag{13}$$

where $\hat{T}_x$ and $\hat{T}_y$ are the commanded torques about the x and y axes respectively and $\hat{\dot{\alpha}}_x$ and $\hat{\dot{\alpha}}_y$ are the desired tilt rates, which can be integrated to give the desired tilt angles. The commanded tilt torque is derived from the spacecraft attitude control loop with feedback from the quaternion error and angular body rates[8]. The input to the motor to control the spin rate of the wheel is the commanded torque about the z-axis with saturation limits applied.

The simplest form of the inner controller decouples the translational and rotational motion of the rotor and has a separate controller for each.

First the Taylor series expansion of the magnitude of the reluctance force is found, ignoring higher order terms, to linearise the system

$$\begin{aligned} F_R &= \frac{\mu_0 N^2 \epsilon l i_0^2}{4\gamma_0^2} + \frac{\mu_0 N^2 \epsilon l i_0}{2\gamma_0^2}\triangle i - \frac{\mu_0 N^2 \epsilon l i_0^2}{2\gamma_0^3}\triangle\gamma \\ &= f_0 + K_i \triangle i - K_\gamma \triangle\gamma \end{aligned} \tag{14}$$

The translational force on the rotor along the x-axis is

$$\begin{aligned} F_x &= f_1 + f_2 - f_5 - f_6 \\ &= 4K_i \triangle i_x + 4K_\gamma \triangle x \end{aligned} \tag{15}$$

Using Newton's Second Law and applying the Laplace Transform, we have the transfer function

$$G_x(s) = \frac{X(s)}{i_x(s)} = \frac{4K_i/M}{s^2 - 4K_\gamma/M} \tag{16}$$

Similarly, for rotation about the y-axis

$$\begin{aligned} T_y &= r_z(f_1 + f_6 - f_2 - f_5) \\ &= 4r_z K_i \triangle i_{\alpha y} + 4r_z^2 K_\gamma \triangle \alpha_y \end{aligned} \quad (17)$$

and assuming the rotor's inertia matrix is diagonal

$$G_{\alpha y}(s) = \frac{A_y(s)}{i_{\alpha y}(s)} = \frac{4r_z K_i / I_{yy}}{s^2 - 4r_z^2 K_\gamma / I_{yy}} \quad (18)$$

The transfer functions for rotation and translation are both double integrators in the range of frequencies of interest with a constant phase angle of -180°. The desired response chosen for the inner controller was 55° of phase margin at a crossover frequency of 100 rads^{-1}. The controller was therefore made from a lead-lag compensator of the form below to generate this phase margin

$$K(s) = K \frac{s+z}{s+p} \frac{s+\omega_i}{\omega_i s} \quad (19)$$

where z and p are the zero and pole of the lead term respectively, and $p > z$. ω_i is the corner frequency of the lag term and K is the loop gain. These terms were tuned to give the desired crossover frequency and the maximum phase margin at this frequency. The crossover frequency was initially chosen to be 100 rads^{-1} for the simulations presented here.

A similar compensator can be derived for the rotational motion. The error between the desired and actual translation or rotation is fed to the input of the compensator and the output is the $\triangle i$ for motion along or about that axis. The current to electromagnet 1 is given below and the currents for the other electromagnets can be derived similarly.

$$i_1 = i_0 + i_x + i_{\alpha y} \quad (20)$$

Because of the $\dot{\alpha} \times I\dot{\alpha}$ term in the rotational dynamics of the rotor there will be a rotational disturbance about the axis normal to the tilt and spin axes. When the angular frequency of the spinning rotor is less than the system's crossover frequency then the controller can damp these disturbances. However, a rotor spinning at 5000 rpm has an angular frequency of 524 rads^{-1} and so the rotor would be unstable. Instead, this gyroscopic disturbance torque can be cancelled using feedback linearisation of the system via a feed forward gain term from the output of the rotor dynamics to the electromagnet current inputs. The torque that the feed forward gain needs to overcome is equal to $\dot{\alpha} \times I\dot{\alpha}$. The mapping from torque to the force that individual electromagnets need to generate is given by finding the pseudo-inverse of the rotational kinematics in Equation 3. The current required by each electromagnet to generate this force is $K_i \triangle i$ from the Taylor series expansion of the reluctance force. Before the feed forward current is added to the current from the controller, when a rotation of the rotor about the x-axis is demanded, the controller drives electromagnets 3, 4, 7 and 8 to tilt the wheel and 1, 2, 5 and 6 to cancel the gyroscopic disturbance. The rotor also becomes uncontrollable when its spin angular velocity exceeds the system crossover frequency. After the addition of the feed forward term, the wheel is stable at all angular velocities and for rotations of the rotor about the x-axis, and the lead compensator outputs only the bias current i_0 for electromagnets 1, 2, 5 and 6

The present simulation of the system uses a continuous-time solver allowing the feed forward term to work at all rotor spin angular velocities. When implemented in hardware, a discrete-time solver will be required. Our hardware set-up implements control loops on a PC running a real-time operating system, with a time step period of 1 ms. With this sampling frequency, the implementation of the feed forward gain will limit the angular velocity of the spinning rotor.

The calculation of the feed forward gain presently uses the rate of tilt about the x and y axes and the spin rate about the z-axis. Hall sensors in the spin motor can be used to calculate the z-axis spin rate. The tilt rates about the other two axes will not be known when the system is implemented in hardware. The angular position is accurately measured by the position sensors and a Kalman estimator has been designed to convert these positions to angular rates.

RESULTS

Simulation Results

Figure 2 shows the attitude of the TopSat spacecraft when it was reorientated through 0.1° by tilting the momentum wheel and also by accelerating the spinning rotor. Because of the larger output torque available from tilting the wheel, this reorientation can be performed almost five times faster than is possible by operating the wheel conventionally. The axis of the output torque

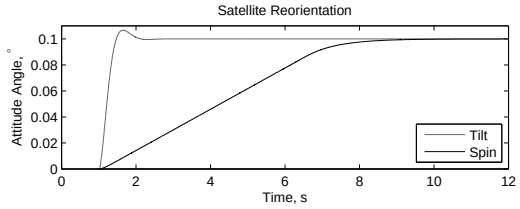

Figure 2: The Satellite's Attitude When Reorientating Using a Tilting Momentum Wheel And a Conventional Momentum Wheel, with the Conventional Torque Limited To a Maximum Value

when tilting the wheel is not fixed and so this torque can be generated about any axis normal to the wheel's spin axis.

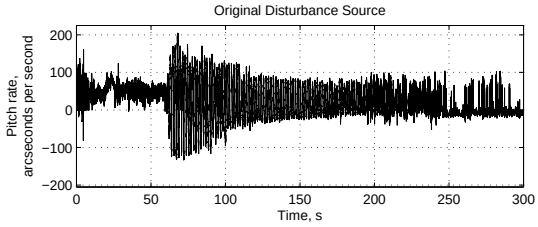

Figure 3: The Attitude Rate Observed on the UK-DMC Satellite While It Was Suffering From a High Frequency Disturbance[10]

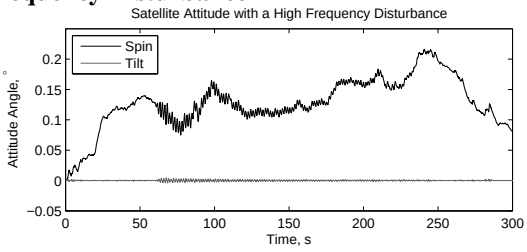

Figure 4: The Satellite's Attitude When Applied with a High Frequency Disturbance Torque That Is Being Damped by a Tilting Momentum Wheel And a Conventional Momentum Wheel

A disturbance in the attitude rates of the UK-DMC spacecraft was identified through image processing[10]. With a frequency of 0.6 Hz the disturbance was too high for the conventional momentum wheels on UK-DMC to damp. The effect of the disturbance is visible in the attitude rate shown in Figure 3. This angular rate data was differentiated to give an angular acceleration and then multiplied by UK-DMC's moment of inertia about that axis to give the torque that caused the disturbance. This torque was then applied to the TopSat model and its attitude is shown in Figure 4 when the disturbance is damped by the momentum wheel operating conventionally and when tilting.

The magnitude of the attitude disturbance is over twenty times less when damped with a tilting momentum-wheel than when it is damped by a momentum wheel operating conventionally. This improvement in performance is due to the tilting momentum-wheel's improved bandwidth.

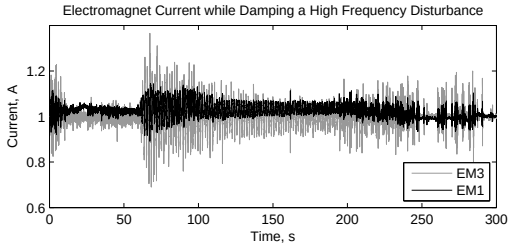

Figure 5: The Current in Two Electromagnets When Damping a High Frequency Disturbance Torque

The disturbance was applied about the x-axis of the spacecraft. Figure 5 shows the current through two electromagnet coils when damping the high-frequency disturbance torque. Because of the gyroscopic nature of the output torque from tilting the rotor, the rotor must be tilted about the y-axis to counteract the disturbance about the x-axis. Electromagnet 1 is one of the four magnets that controls the tilt of the wheel about the y-axis. The varying current in electromagnet 3 is due to the current required by the feed forward term in the controller. This feed forward term prevents any gyroscopic motion of the rotor. Preventing the gyroscopic motion of the rotor transfers the gyroscopic torque produced to the spacecraft to generate the tilting component of the output torque T'.

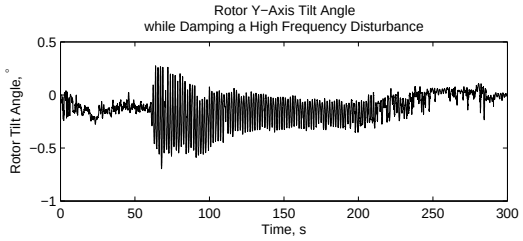

Figure 6: The Rotor Tilt Angle When Damping a High Frequency Disturbance Torque

Figure 6 shows how the tilt angle of the rotor about the y-axis varies as the earlier disturbance torque is damped.

The frequency response of the entire spacecraft attitude when controlled using a tilting momentum-wheel and a conventional momentum-wheel was measured using

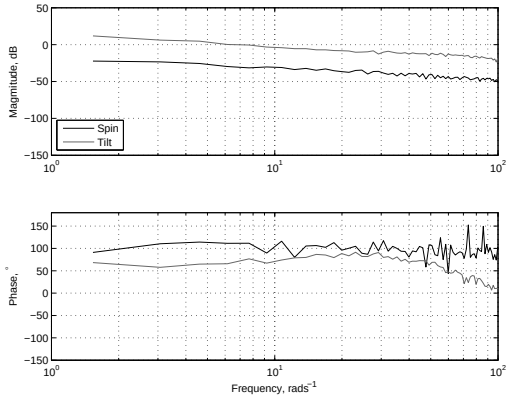

Figure 7: The Frequency Response of a Tilting And a Conventional Momentum Wheel

a Dynamic System Analysis (DSA) tool developed by the authors. A white-noise disturbance was injected into the attitude control loop and the system's response was recorded. The bode plot of the response is shown in Figure 7. When controlled with the tilting momentum wheel the crossover frequency of the system is at 6 rads^{-1}. The crossover frequency of the conventional wheel system is two orders of magnitude less.

From Equations 15, 17 and 20, for every translation or rotation movement there will be an increase in the current through one electromagnet and an equal decrease in the current through another electromagnet. These will cancel and so therefore, the total current for all eight electromagnets at all times with this decoupled controller is eight times the bias current.

Experimental Results

An engineering model of the 3Dwheel has been built and is currently being tested to verify its simulated properties and to allow the development of controllers. The results presented in this section are the initial results from this testing. Figure 1 shows a photograph of the wheel. The stator electromagnets are built from laminated steel with a curved pole face accurately cut using wire erosion. The position and tilt angle of the wheel is measured by contact free eddy current sensors, which measure the position of an aluminium liner inside the steel rotor to an accuracy of 2 μm. Low noise current amplifiers were built from linear audio amplifier ICs. The controller was implemented on a PC running a real time operating system sampling at 1 kHz.

The DSA tool was used to calculate the frequency response of the amplifier and electromagnets. This response was combined with the numerical model of the translation and rotation dynamics and the anti-aliasing filters, to derive a controller. The controller variables were adjusted to give the maximum phase margin at the system's crossover frequency.

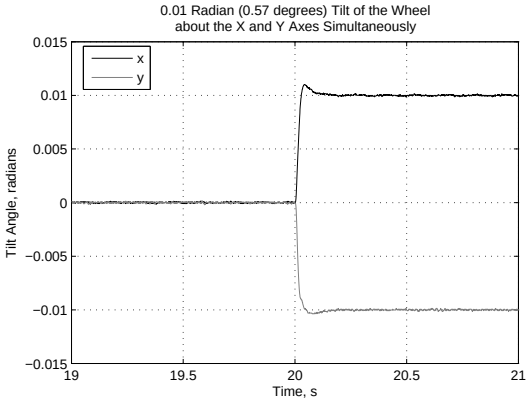

Figure 8: A Rotation Step Response with the Axis of Rotation Between the Wheel's Principle Axes

Figure 8 shows the response of the wheel to a step command for a rotation about an axis between the wheel's x and y principle axes. The electromagnets are aligned with the x and y principle axes. This plot demonstrates that it is possible to tilt the wheel about any axis on the plane normal to the wheel's spin axis and therefore to generate a torque about any axis on this plane. Experiments show that the translation loop is decoupled from the rotation loop by at least -46 dB up to the crossover frequency.

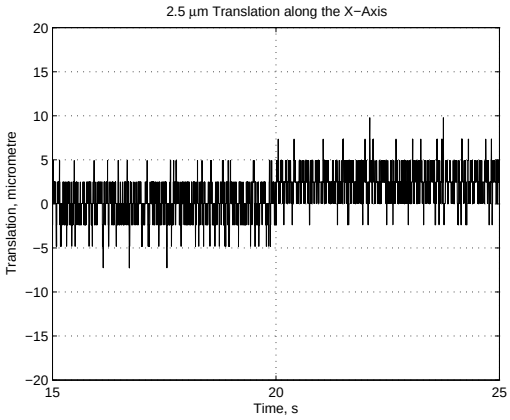

Figure 9: The Response To a 2.5 micrometre Translation Step Command along the x-axis

Figure 9 shows the wheel's response to the step command for a 2.5 micrometre translation along the positive x-axis at time 20.0 seconds. The data acquisition card used in the engineering model has a 12-bit resolution,

with the least significant bit corresponding to a translation of 2.4 μm. The quantisation of the position is visible showing that the wheel can be controlled with a very high precision, with the engineering model's precision being limited by the resolution of the data acquisition card.

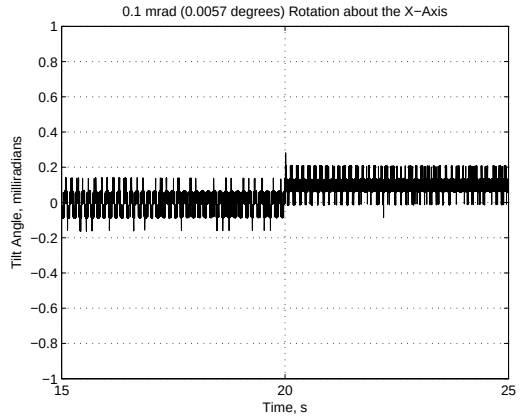

Figure 10: The Response To a 0.1 milliradian Rotation Step Command about the x-axis

Figure 10 shows the wheel's response to the step command for a 0.1 milliradian (0.0057°) rotation about the x-axis. Again the resolution of the 12-bit data acquisition card is defining the resolution that the wheel can be tilted with.

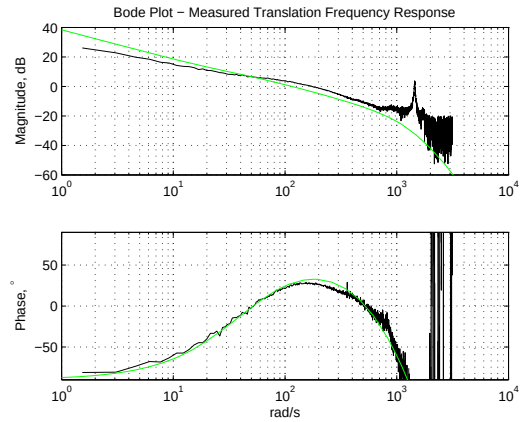

Figure 11: The Measured (Black) and Simulated (Green) Frequency Response of the Loop Transfer Function of the Decoupled Translation Controller and Dynamics

Figure 11 shows the measured and simulated frequency response of the loop transfer function of the initial decoupled rotation controller and plant dynamics. The simulated model gives a good phase match at lower frequencies. The cross over frequency of the measured system is 176 rads^{-1} with a phase margin of 28°.

The wheel can be tilted at a rate of 1.0 rads^{-1} allowing a gyroscopic torque of 1.2 Nm to be generated. The tilt rate is determined by the speed of the controller. The controller can be made faster. Increasing the tilt rate will allow the same magnitude of gyroscopic torque to be generated with the wheel spinning at lower rates.

CONCLUSION

We propose a novel concept for 3-axis attitude control of a spacecraft using a single momentum wheel that uses an active magnetic bearing. Using an active magnetic bearing allows a momentum wheel for spacecraft attitude control to be made with improved properties compared to a wheel that uses conventional bearings. The use of active magnetic bearings allows a single wheel to generate an output torque about all three axes of the spacecraft. A conventional output torque can be generated about the spin axis of the wheel and a gyroscopic torque can be generated about any axis on the plane normal to the spin axis. Because the gyroscopic torque is generated by tilting the wheel it has a high bandwidth, and because its magnitude is proportional to the tilt rate its magnitude can be high. The simulated properties of the wheel have been successfully demonstrated by the engineering model of the wheel that has been built.

Acknowledgements

The authors would like to thank The Nuffield Foundation for their partial support of this project with grant NAL/32791.

References

1. Murakami, C., Y. Ohkami, O. Okamoto, A. Nakajima, M. Inoue, J. Tsuchiya, K. Yabu-Uchi, S. Akishita and T. Kida, "A New Type of Magnetic Gimballed Momentum Wheel And Its Application To Attitude Control in Space," Acta Astronautica, vol. 11, no. 9 613–619, 1984.

2. Scharfe, M., K. Meinzer and R. Zimmermann, "Development of a Magnetic-Bearing Momentum Wheel for the AMSAT Phase 3-D Small Satellite," in International Symposium on Small Satellites, Annecy, France, 1996, no. A97-23887.

3. Scharfe, M., T. Roschke, E. Bindl, D. Blonski and R. Seiler, "The Challenges of Miniaturisation For a Magnetic Bearing Wheel," in Proceedings of the 9th European Space Mechanisms and Tribology Symposium, (editor) R. A. Harris, pages 17 – 24, Liege, Belgium, 2001.

4. Gerlach, B., M. Ehinger, H. K. Raue and R. Seiler, "Gimballing Magnetic Bearing Reaction Wheel With Digital Controller," in 11th European Space Mechanisms and Tribology Symposium, ESMATS 2005, (editor) B. Warmbein, pages 35 – 40, ESA, Lucerne, Switzerland, 2005.

5. Sindlinger, R., "Magnetic Bearing Momentum Wheels with Magnetic Gimballing Capability for 3-Axis Active Attitude Control and Energy Storage," in Attitude and Orbit Control Systems Conference, vol. ESA SP-128, pages 395–401, European Space Agency, Noordwijk, 1977.

6. D'Arrigo, A. and A. Rufer, "Integrated Electromagnetic Levitation and Guidance System for the Swissmetro Project," in International Conference on Magnetically Levitated Systems, pages 263–268, Rio de Janeiro, Brazil, 2000.

7. Sidi, M. J., Spacecraft Dynamics And Control : A Practical Engineering Approach, Cambridge University Press, 1997.

8. Pechev, A. N., "Feedback-Based Steering Law For Control Moment Gyros," Journal of guidance, control, and dynamics, vol. 30, no. 3 848–855, 2007.

9. Genta, G., Dynamics of Rotating Systems, Springer, New York, 2005.

10. Bamber, D. C., D. P. L. Palmer and D. S. Mackin, "Attitude Determination through Image Registration Model and Test-case for Novel Attitude System in Low Earth Orbit," in AIAA/AAS Astrodynamics Specialists Conference, pages 1–14, Keystone, Colorado, 2006, no. AIAA 2006-6157.